Numerical Study of Jet Impingement on Heated Sink Covered by a Porous Layer

Mohammed A. Thani [1, *], Muneer A. Ismael [2]

[1, 2] *Department of Mechanical Engineering, College of Engineering, University of Basrah, Basrah, Iraq*
E-mail addresses: mohammed7dec88@gmail.com , muneer.ismael@uobasrah.edu.iq
Received: 27 February 2022; Revised: 28 March 2022; Accepted: 5 April 2022; Published: 24 December 2022

Abstract

This numerical study aims to enhance the heat transfer efficiency by dissipating the heat Emitted from electronic processors. A jet impingement technique is utilized with porous layer covering a metal fin as a heat sink. Forced convection and normal convection (due to the buoyancy effect) are taken into consideration. The two equations model (Local Thermal Non-Equilibrium LTNE) employed to describe the energy equations of the two phases of the porous surface. Finite Element Method (FEM) used to discretize these equations to obtain the numerical solution. To make this study closest to the reality, constant heat flux boundary condition is applied underneath the metallic heat sink. The geometry comprises of three domains: Free flow channel, Porous layer and Metal fined heat sink. In order to simulate the heat transfer, isotherms; streamlines and Nusselt number have been considered. Investigation has been done by inspecting the effects of the pertinent non-dimensional parameters such as: Reynolds number (Re = 100-900), Darcy number ($Da = 10^{-1}$-10^{-6}), Richardson number (Ri = 0.1-100) and Porosity (ε = 0.85-0.95). The results show that increasing Re and decreasing ε lead to enhance Nusselt number. Richardson number below 100 has no significant effects on Nu. At Re above 400, Nusselt number proportional with Darcy number. The enhancement of Nusselt number is found to be 250 % by increasing Re from 100 to 900, 290 % by decreasing ε from 0.95 to 0.85 and about 13 % by increasing Darcy number from 10^{-6} to 10^{-1}.

Keywords: Darcy Forchheimer, Jet impinging, LTNE, Laminar flow, Heat sink, Porous media.

1. Introduction

The common method which employed for providing high local heat transfer and cooling a wide range of engineering and industrial applications is Jet Impingement [1]. This Technique is used for cooling metals, blades of turbine, electronics equipment, glass tempering, textiles drying, anti-icing, etc. [2-14]. Hussein et al. [15] investigated a confined slot jet impinging a porous block filled trapezoidal cavity. They discovered that the preferred thickness of the porous layer as minimum as possible.

Free convection due to buoyancy force induced by high heat flux is flowing against the direction of the jet slot. It leads to mixed convection (Forced and Free) [16], [17] and this case happen in natural and technological process. Buonomo et al. [18] examined numerically the mixed convection by a slot jet impinging a metallic foam-covered parallel plate heated channel. Their findings at low Peclet numbers showed heat transfer decrement, while it increases at high Peclet numbers, as well as porosity influences insignificant on average Nusselt number.

Adding of metal fins or baffles increase the surface area for heat exchanges which in turn boosts the heat exchange. Recently, another technique for Heat dissipation enhancement is by using porous media such as metallic foam due to its high thermal conductivity. It used in many engineering applications like: crude oil extraction, porous bearing, nuclear reactors,

thermal insulation, etc. Jeng et al. [19] studied confined slot jet impinging to cool an aluminum foam as a heat sink. They concluded that metal foam existence promotes the heat transfer 2-3 times and reduce the thermal resistance by 30 %. It is prevailed that mixed convection mode might cause minimum heat transfer unfavorably due to counteraction of jet flow against buoyancy driven flow. Minimum mean Nu occurred more obviously at higher values of the height of the porous layer. Thus, the design of jet impingement cooling through porous medium must be carefully considered in the mixed convection regimes [20]. To describe flow in porous media, the extended Darcy-Forchheimer-Brinkman model is commonly used. With the addition of a porous layer at $Da = 10^{-2}$, recirculating foaming on heat sources are entirely avoided. The magnitude of overall heat transfer and momentum friction increases with increasing Da. The free convection was observed in dead zones making the entire system is partially mixed convection [21]. This instance when Nu exhibits a minimal value is not visible for low levels of Ra or thermal conductivity ratio. With those factors held constant, it is discovered that narrower solid objects have significantly higher Nusselt numbers. As a consequence, the computational findings show that for cooling purposes, the solid wall should be as thin as feasible and have a high thermal conductivity. The chilling rate is slower inside the opposing missing convection mode than the natural convection form (where the free convection is the main mechanism criteria) [22]. The metal

foam porous media enhances heat transfer surface area making better heat transfer characteristics for higher porosity beside the turbulence generation [23]. The increasing of pores in unit of area enhances heat transfer significantly for higher values of void fraction [24]. The adding of longitudinal fins to a heat sink improves heat transmission dramatically while incurring just a little pressure decrease. When thermal layers between neighboring fins combine and then become virtually formed for most of the height of something like the heat sink, convective amplification is maximized [25]. When metal foams are inserted, the pressure drop is substantially greater than when finned heat sinks are used. The heat transfer performance of finned metal foams is superior to that of a traditional heat sink with much the same number of fins. Finned copper foaming heat sinks have application possibilities in some constrained and narrow locations, even with higher flow resistance, when pump energy consumption is not the primary factor [26].

Recently, metallic foam with fins impinging by air jet has received a great attention due to its use in many technologies to boost heat transfer dissipation from the heat source. Gibanov et al. [17] achieved simulation studies to investigate mixed convection inside a rectangular chamber with a triangle porous medium and a regional heater. The non-dimensional stream functional and vorticity formulation was used to solve the fundamental differential equation with associated constraints using the finite difference technique. The effects of the Richardson number ($Ri = 0.01 - 10$) and Darcy numbers ($Da = 10^{-7}$ to 10^{-1}) on streamlines and isotherm models, as well as the mean and local Nusselt number at the heaters, have indeed been investigated. Every one of these critical aspects has been shown to have a significant impact. Jasim [27] studied the effect of fluid-structure interactions in managing convective heat transfer within a ventilated horizontal channel with elastic materials utilizing simulation studies. A bendable slender fin was affixed to a cavity's lower surface. Water with a Prandtl number of 5.8 penetrated the rectangular cavity through an entrance in the bottom side of the left vertical surface and escapes through an aperture inside the upper portion of the left vertical wall. The controlling mathematical models of computational fluid dynamics and solid mechanics, which also include consistency, velocity, heat, and dislocation, were solved with the help of COMSOL Multiphysics software version 5.2 as well as the Galerkin finite element put in place in the arbitrarily defined Eulerian-Lagrangian (ALE) approach. The results revealed that at larger Cauchy and Richard values, the fin form and local Nusselt value achieve a reliable estimate condition. This research also found that utilizing a flexible fin enhanced heat transmission, with an increase in average Nusselt number of between 10.45 % and 230 % when comparing with using the same stiff fin or without a fin. Yaseen and Ismael [28], focused on the simulation of non-Newtonian fluid inside an extended trapezoid container, Fluid-Structure Interaction (FSI) and coupled convective heat transfer. Within the laminar area, a non-Newtonian is examined. An iso-thermal heated hollow base panel simulates the heating element, while the remainder of a wall surface was properly insulated. A flexible barrier was fastened to a channel's top portion, with its free end extending into the air passage. The flexible baffle's position on the top wall varies. The Richardson value (0.01 to 100) or simple linear indices (0.5 to 1.5) are used to analyze the barrier location. The issue was addressed to use the finite element model and the ALE

methodology (Arbitrary Lagrangian-Eulerian). The findings correspond to the channel that isn't perplexed. The proposed baffled channel significantly improves heat transmission, according to the research. Abd Al-Hassan [29] studied convective heat transfer in a composites horizontal passage coupled to a square cavity computationally. The permeable barrier was restricted by the hollow, which was made up of an interfacial material on the base and a flowing sheet on top. Numerical simulation method based on physics program. The $Pr = 6.26$, $Da = 10^{-3}$, the buoyancy ratio = 0.5, the Lewis values $Le = 20$, and the gravity diffusion coefficient ratio = 0.533 are all set in constant values. The issue was comprised of 4 variables: the Reynolds number = 50 to 250, the Richards number = 0.01-100, the depth of the porous material $Hp = 0.25-1$, and the tilt of a foam interface. For two situations of heating and variety suppliers, all four variables were replicated (opposing and assisting cases). The results indicated that when the sources are put on the aiding side, maximal heat transfer occurs, whereas lowest heat transfer occurs whenever the supplies are set on the opposite site. The study demonstrated that whenever the supplies were put mostly on aiding part, maximal heat transfer occurs, whereas lowest heat exchange occurs when the sources are set on the opposing side. At $Re = 50$ and 250, the percentage change in Nusselt numbers between both the opposing and assisting instances was 53.07 percent and 90.184 percent, correspondingly, for $Ri = 0.01$. At $Re = 50$ or 250, the percent changed in Nu average for the opposite situations is 36.30 percent and 17.81 percent, correspondingly, for $Ri = 100$.

The purpose of this research is to study and explore the influence of the mixed convection using air slot jet impinging on a metallic fin heat sink filled by metallic foam when no thermal equilibrium exists. High quality hypothesis is taking under consideration to make the simulation as reach as possible to the actual operation.

2. Mathematical representation

The problem under investigation is a finned heat sink attached to a heat source and placed in a horizontal channel. Air is impinging into the heat sink via a slot jet made in the upper wall of the channel and discharges out from the two open ends of the channel. To enhance the dissipation of heat from the sink, a porous material is inserted within the heat sink as shown in Fig. 1. The heat transfer within the porous layer is modeled based on the local thermal non-equilibrium thus, the porous media requires two energy equations for solid matrix and fluid flow within it. The heat flux is introduced through the base of heat sink. The normal width is considered too long thus, the problem is taken as two dimensional. The fluid is considered incompressible and Newtonian while the flow is kept within the laminar region. The problem is solved transiently and the properties are taken constant (except the change of the density due to temperature variety) fluid will be consider. Local thermal Non-Equilibrium (LTNE) by using two energy equations, one for fluid and the second for solid phase utilize to describe the energy equations of the porous layer [30], [31]. Constant heat flux on the heat source is assumed.
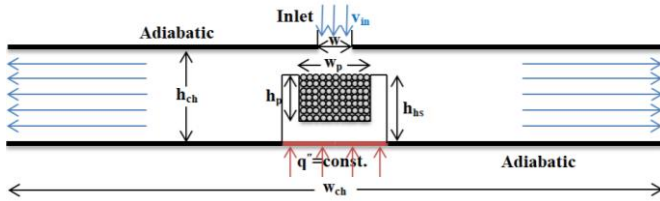
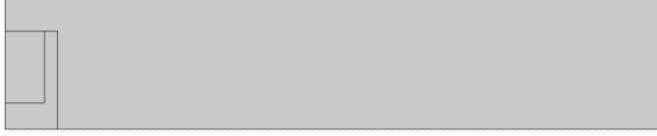**Fig. 1** Physical domains (2 dimensions).

Fig. 2 Computational domain.

For the fluid flow uses continuity and momentum Navier-Stokes extended with Darcy-Brinkman Forchheimer model to describe the pressure drop in porous layer.

Because of the symmetric, one-half of the geometry will be simulated to reduce the time of the run. Dimensionless parameters like: Reynolds number (Re), dimensionless permeability K (Da), porosity (ε), Richardson number (Ri), foam thickness (Hp), solid to fluid thermal conductivity (σ) and jet slot width (W) effect the Nu and pressure difference.

The used momentum equation can be divided into two categories: flow in an open channel and flow in void space inside the porous media domain as shown in the following dimensionless expressions:

- Momentum equation of fluid on free stream channel (open channel) in x and y axis respectively:

$$\frac{\partial U}{\partial \tau} + U\frac{\partial U}{\partial X} + V\frac{\partial U}{\partial Y} = -\frac{\partial P}{\partial X} + \frac{1}{Re}\left(\frac{\partial^2 U}{\partial X^2} + \frac{\partial^2 U}{\partial Y^2}\right) \tag{1}$$

$$\frac{\partial V}{\partial \tau} + U\frac{\partial V}{\partial X} + V\frac{\partial V}{\partial Y} = -\frac{\partial P}{\partial Y} + \frac{1}{Re}\left(\frac{\partial^2 V}{\partial X^2} + \frac{\partial^2 V}{\partial Y^2}\right) + Ri\ \theta_f \tag{2}$$

- Momentum equation of voids porous media:

$$\frac{1}{\epsilon}\frac{\partial U}{\partial \tau} + \frac{1}{\epsilon^2}\left(U\frac{\partial U}{\partial X} + V\frac{\partial U}{\partial Y}\right) = -\frac{\partial P}{\partial X} + \frac{1}{\epsilon Re}\left(\frac{\partial^2 U}{\partial X^2} + \frac{\partial^2 U}{\partial Y^2}\right) - \frac{1}{Re\ Da}U - \frac{Cf}{\sqrt{Da}}|U|U \tag{3}$$

$$\frac{1}{\epsilon}\frac{\partial V}{\partial \tau} + \frac{1}{\epsilon^2}\left(U\frac{\partial V}{\partial X} + V\frac{\partial V}{\partial Y}\right) = -\frac{\partial P}{\partial Y} + \frac{1}{\epsilon Re}\left(\frac{\partial^2 V}{\partial X^2} + \frac{\partial^2 V}{\partial Y^2}\right) - \frac{1}{Re\ Da}V - \frac{Cf}{\sqrt{Da}}|U|V + Ri\ \theta_p \tag{4}$$

The heat transfer mechanisms in present system consists of: (i) convection in free stream channel and porous media, (ii) heat conduction through finned wall and (iii) heat conduction through porous media matrix as shown below:

- Heat Transfer in Fluid

- In free stream channel

$$\left(\frac{\partial \theta_f}{\partial \tau} + U\frac{\partial \theta_f}{\partial X} + V\frac{\partial \theta_f}{\partial Y}\right) = \frac{1}{Pe}\left(\frac{\partial^2 \theta_f}{\partial X^2} + \frac{\partial^2 \theta_f}{\partial Y^2}\right) \tag{5}$$

- In voids of porous media

$$\frac{\partial \theta_f}{\partial \tau} + \frac{1}{\epsilon}\left(U\frac{\partial \theta_f}{\partial X} + V\frac{\partial \theta_f}{\partial Y}\right) = \frac{1}{Pe}\left(\frac{\partial^2 \theta_f}{\partial X^2} + \frac{\partial^2 \theta_f}{\partial Y^2}\right) + \frac{H_v}{\epsilon\ Pe}(\theta_s - \theta_f) \tag{6}$$

- Heat conduction in matrix of porous media

$$\frac{\partial \theta_s}{\partial \tau} = \frac{\gamma_1\ \sigma_1}{Pe}\left(\frac{\partial^2 \theta_s}{\partial X^2} + \frac{\partial^2 \theta_s}{\partial Y^2}\right) + \frac{\gamma_1\ H_v}{(1-\epsilon)Pe}(\theta_f - \theta_s) \tag{7}$$

- Heat conduction in finned wall

$$\frac{\partial \theta_{hs}}{\partial \tau} = \gamma_2\ \sigma_2\ \frac{1}{Pe}\left(\frac{\partial^2 \theta_{hs}}{\partial X^2} + \frac{\partial^2 \theta_{hs}}{\partial Y^2}\right) \tag{8}$$

The utilized boundary conditions of momentum and heat transport equations are:

1. Inlet ($0 \leq X \leq 1$, $Y = H_{ch}$): $U_{in} = 0$, $V_{in} = -1$, $\theta = \theta_f = 0$

2. Outlet ($X = \pm W_{ch}/2$, Y): $P_{out} = 0$, $\partial\theta/\partial X = 0$

3. Insulated walls ($1 < X \leq W_{ch}/2$, $Y = H_{ch}$): $U, V = 0$, $\partial\theta/\partial Y = 0$

4. Interface surface between fluid and solid matrix: $\theta_f = \theta_s$

5. Interface surface between fluid and Heat sink: $\theta_f = \theta_{hs}$
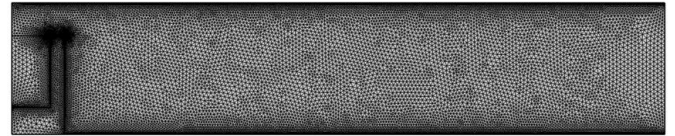
6. Heat sink's base $\partial\theta/\partial Y = -1$

Fig. 3 The mesh distribution of present study.

Mesh optimization is an essential step to be considered when using the any descripted numerical method. To handle the model solution with a large number of mesh components, the physical memory of the personal computer requires more time, and it is necessary to fine-tune the most accurate mesh with a shorter solving time. In the current study, we sued the finite element method. The optimal mesh element counts in the current study are 50000 mesh elements. As shown in Fig. 4, the Nu number value of 50000 mesh numbers is near to 70000 and 120000 mesh numbers, which require more time to achieve the answer.
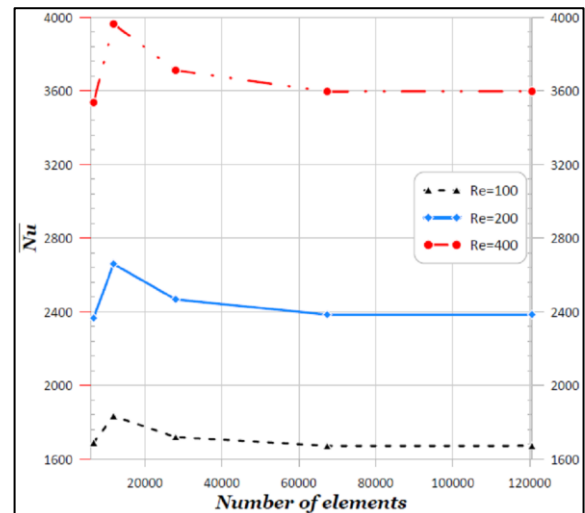

Fig. 4 the mesh optimization of present study.

The conservation equations are converted from complex PDE system into simpler algebraic system by using Finite Element Method (FEM). A matrix system is generated by making momentum and heat balance upon every single element of mesh distribution making the large number of simultaneous algebraic equations equals to number of mesh elements number. The solution is achieved when the tolerance error is approached to a specified error (for present work 0.1 % is satisfied). The momentum equations matrix is solved firstly based on the reference temperature for the whole flow domains, the heat transfer of the three domains is connected to each other by boundary conditions of different mechanisms where the momentum result is customized to the convection part of heat transfer in fluids, the resultant solution will be applied on momentum system to modify the physical properties, and so on as shown in Fig. 5.
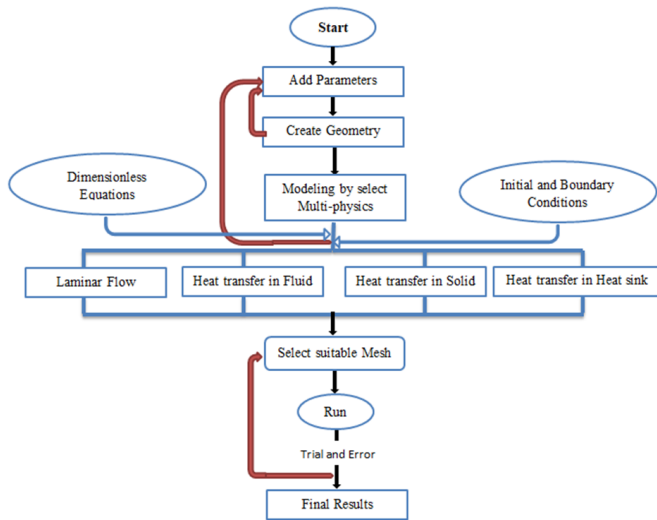

Fig. 5 the finite element method procedure for present system.

Richardson number represents the rate of natural convection to the forced convection:

$$Ri = \frac{Gr}{Re^2} \qquad (9)$$

Grashof Number is the ratio of the buoyancy forces to viscous forces, *Gr* is a function to the physical properties of fluid, gravity, the temperature difference between the hot surface and bulk fluid and the characteristic length as illustrated in the follows:

$$Gr_x = \frac{g\,\beta\,\rho^2(T_w - T_\infty)\,x^3}{\mu^2} \qquad (10)$$

Where β is the thermal expansion coefficient, which is intensive thermodynamic property [32] given by:

$$\beta = -\frac{1}{\rho}\left(\frac{\delta\rho}{\delta T}\right)_P \qquad (11)$$

For practical analysis and calculations, *T* is taken as the average value of hot surfaces and bulk fluid which is called film temperature (T_f) [33]. The physical properties are taken at film temperature for the entire system calculations.

Prandtl number (*Pr*) is the ratio of momentum diffusivity to thermal diffusivity, every single material and fluid has its *Pr*. Prandtl number can be calculated by the following expression:

$$Pr = \frac{Cp\,\mu}{K} \qquad (12)$$

Rayleigh number (*Ra*) is the multiple forms of Grashof number and Prandtl number which are given by:

$$Ra_x = Gr_x\,Pr = \frac{Cp\,\mu}{K} \cdot \frac{g\,\beta\,\rho^2(T_w - T_\infty)\,x^3}{\mu^2}$$

$$Ra_x = \frac{g\,\beta\,\rho^2\,Cp\,(T_w - T_\infty)\,x^3}{\mu^2\,K} \qquad (13)$$

The Rayleigh number is an indication of the turbulence intensity of natural convection, the critical value of *Ra* number is the limit of laminar flow development. In other words, if the *Ra* becomes higher than the critical value (109), the unstable behavior of natural convection due to turbulence or boundary layer interactions would be happened [34].

The heat system operation configurations (isothermal or constant heat flux) and orientations of the system (vertical or horizontal) [33]. For constant heat flux, *Gr* is replacing by *Gr** which is obtained by following:

$$Gr^* = Gr\,Nu \qquad (14)$$

Then,

$$Ra^* = Gr\,Pr \qquad (15)$$

For forced convection Reynolds number is applied, which means the ratio of inertial forces to viscous forces. The Reynolds number can be expressed as following:

$$Re = \rho\,d\frac{v}{\mu} \qquad (16)$$

For mixed convection Richardson number is applied which can be expressed as:

$$Ri = \frac{Gr^*}{Re^2} \qquad (17)$$

When *Ri* goes to zero, the forced convection is the major mechanism in bulk fluid, and if it goes to infinity, the free convection mechanism is the major. For porous media, Darcy's number is applied, which means the ratio of relative porous media permeability to square power of characteristics length such as particle diameter, it can express as following:

$$Da = \frac{K}{d^2} \qquad (18)$$

The *Da* has direct effect on heat transfer through porous media, high values mean high pores per unit length and vice versa.

Nusselt number (*Nu*) is the ratio of conductive heat transfer resistance to convective heat transfer resistance, given by the following expression:

$$Nu_x = \frac{h_x}{K} \qquad (19)$$

Where $h = q/(T_w - T_b)$, heat transfer coefficient equals to the ratio of heat flux to temperature difference between solid wall and bulk fluid.

The calculated local Nusselt number is:

$$Nu = \frac{-\left(\epsilon \frac{\partial \theta_f}{\partial Y} + (1-\epsilon)\,\sigma_1 \frac{\partial \theta_s}{\partial Y}\right)}{\theta_w} \qquad (20)$$

Where the first and the second terms represent fluid and solid phases respectively:

$$Nu_f = \frac{\epsilon \frac{\partial \theta_f}{\partial Y}}{\theta_w} \qquad (21)$$

$$Nu_s = \frac{(1-\epsilon)\,\sigma_1 \frac{\partial \theta_s}{\partial Y}}{\theta_w} \qquad (22)$$

The average Nu number below the porous layer:

$$\overline{Nu} = \frac{1}{S_1} \int_0^{S_1} Nu\, dx \qquad (23)$$

$$\overline{Nu} = \frac{1}{S_2} \int_0^{S_2} Nu\, dy \qquad (24)$$

Where: $S_1 = Wp$ and $S_2 = Hp$

3. Results and Discussions

This section displays the dimensionless results graphically. It is necessary to enhance the confidence level of the used numerical technique. Therefore, a comparison was made with Hussein et al. [15]. The present investigation has excellent validation, where the Nusselt number of present work value is close to previous work as shown in Fig. 6. Nusselt number vs. Re for various porous media height plots are illustrated in Fig. 6. The validation percent is close to 99.9 % for whole Re and Hp.
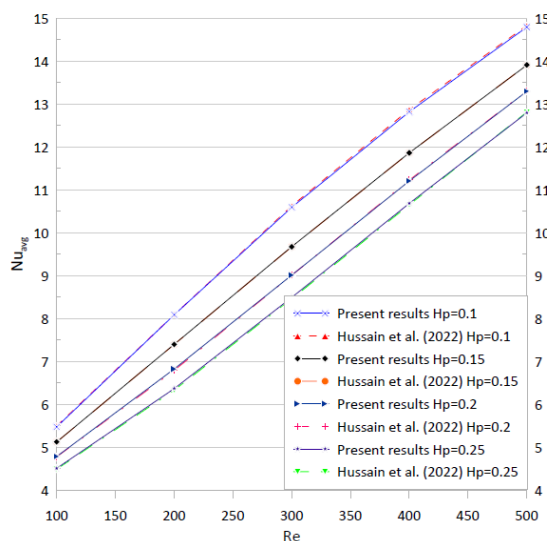

Fig. 6 Validation of the present work by comparing with average Nu of Hussein et al. [15] for $Re = 100\text{-}500$, $Hp = 0.1\text{-}0.25$, $\varepsilon = 0.75$, $Da = 10^{-3}$.

Table 1. illustrate the percentage error of average Nusselt number for the present work with Hussein et al. [15]. The validation shows a great matching between both results and the percentage of error doesn't exceed 0.6 %.

Table 1. Percentage of error of average Nu between the present work and Hussein et al. [15] for $Re = 100\text{-}500$, $Hp = 0.1\text{-}0.25$, $\varepsilon = 0.75$, $Da = 10^{-3}$.

Re	$Hp = 0.1$	$Hp = 0.15$	$Hp = 0.2$	$Hp = 0.25$
100	- 0.44268	- 0.39923	0.131929	0.393602
200	- 0.03594	- 0.23341	0.437518	0.534662
300	- 0.30431	- 0.12117	- 0.00632	0.328478
400	- 0.39552	- 0.27332	- 0.19947	0.288688
500	- 0.25048	- 0.30541	- 0.04907	- 0.14452

The progress of streamlines depicted in Fig. 7 shows no intensified vortices by increasing Re through the present system. The high Re is prevailed by high velocity distribution, the inertial forces due to velocity increasing overcomes the viscous forces. The streamlines of thinner or distracted boundary layer are indicated for higher Re. The fluid seems to be stagnant at $Re = 100\text{-}400$ in porous media domain. The fluid starts to circulate within the porous domain by increasing Re above 400 and the maximum fluid circulation presents within $Re = 900$ as an indication to the dominant inertial force.
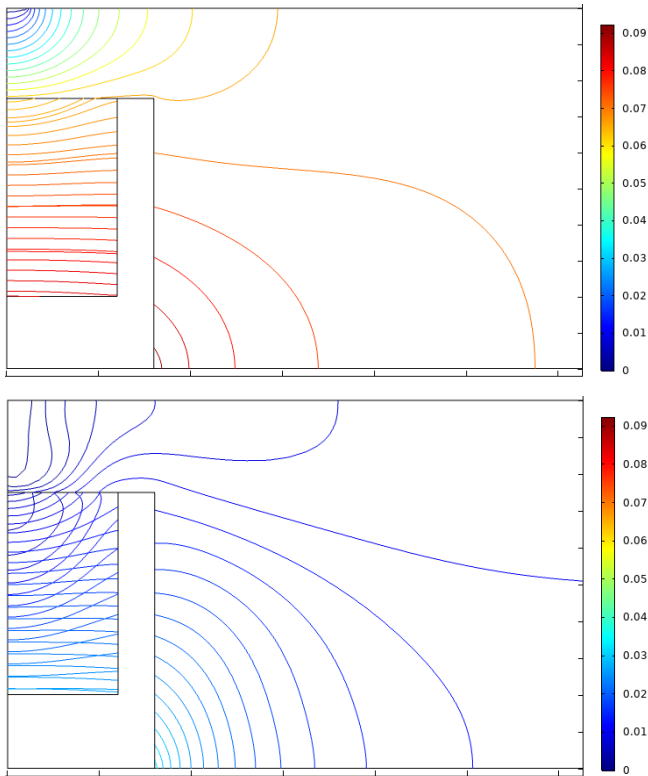

$Re = 100$

$Re = 200$

$Re = 400$

$Re = 900$
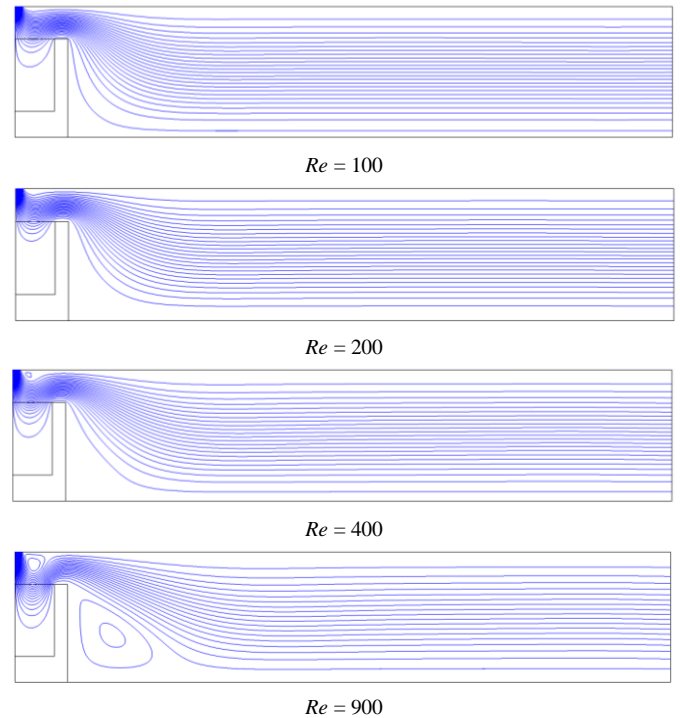
Fig. 7 Streamlines for $\varepsilon = 0.85$, $Ri = 10$, $Da = 10\text{-}3$, $Pr = 0.71$, $\sigma_{1,2} = 8080$ and $\gamma_{1,2} = 5 \times 10^{-4}$ on various Re.

Fig. 8 shows the temperature distribution for various Reynolds numbers. The increase of Re shows a uniform distribution of temperature distribution. The warmer heat sink and porous media are shown in $Re = 100$ and the cold ones are shown in $Re = 900$. The increasing of Re of the inlet cold fluid makes the high amount of cold fluid to deal with hot fluid volume enclosed by heat sink and porous media. The cold and hot fluid particles are mixed effectively by increasing Re. The thermal boundary layer is distracted by momentum boundary layer destruction where the temperature distribution is in harmonic fashion with streamline results.
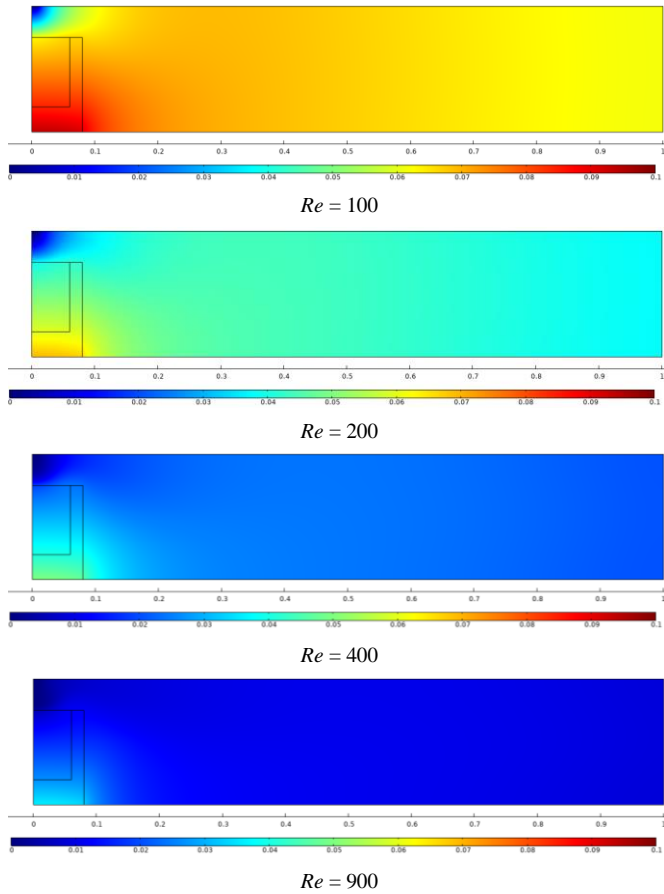
Fig. 8 Temperature profile for $\varepsilon = 0.9$, $Ri = 10$, $Da = 10^{-3}$, $Pr = 0.71$, $\sigma_{1,2} = 8080$ and $\gamma_{1,2} = 5 \times 10^{-4}$ of various Re.

Fig. 9 reveals the temperature gradient for the porous layer phases (solid and fluid) and how it approximately reaches the thermal equilibrium after passing time period.

Fig. 9 Isotherm contour for (fluid and solid phases) for $Ri = 10$, $Da = 10^{-3}$, $Pr = 0.71$, $\sigma_{1,2} = 8080$ and $\gamma_{1,2} = 5 \times 10^{-4}$ and $\varepsilon = 0.90$, $Re = 100$-900 respectively.

Average Nusselt number at low values of Reynolds number (less than 400) doesn't affect by various Richardson number values. Little influence appears at $Re > 400$ when $Ri = 100$, it shows decrease in average Nusselt number due to high natural convection overcome the forced convection in porous media domain. The Nu increases by increasing Re, while the Ri has marginal effect on Nu at lower Ri (bellow $Ri = 100$).

Fig. 10 presents the average Nusselt number (solid and fluid phases) with Reynolds for various Darcy number in porous media domain. The Nu increases by increasing Re, while the Da has marginal effect on Nu at lower Re (bellow $Re = 400$). Nevertheless, at $Re > 400$, the increase in permeability or Darcy number boosts the heat transfer coefficient due to high penetration of the air jet throughout the metal foam, a significant increase in Nu can be observed. The maximum percentage increase of average Nusselt number is about 13.267 % at $Re = 900$ due to Darcy number variation from 10^{-6} to 10^{-1}.
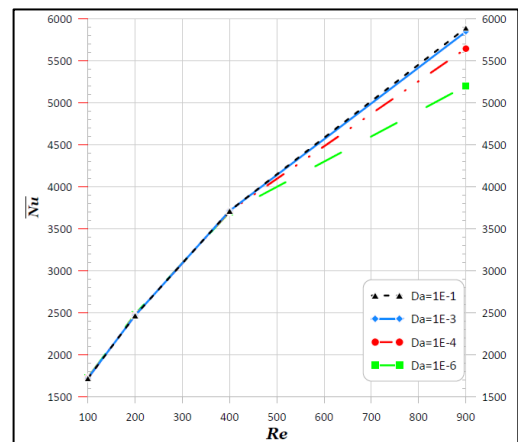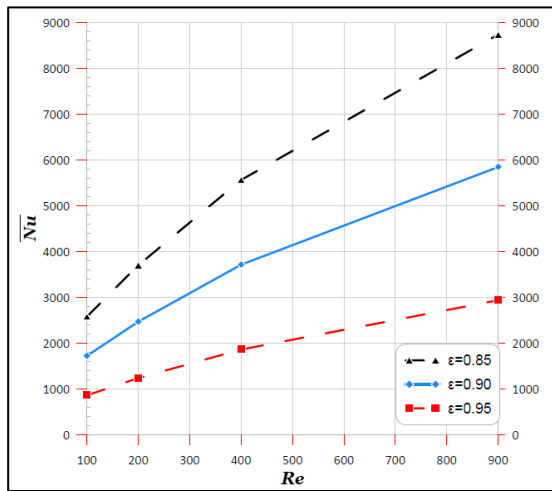

Fig. 10 Average Nu (fluid and solid phase) with Re for various Ri in porous media domain $\varepsilon = 0.9$, $Da = 10$-3, $Pr = 0.71$, $\sigma_{1,2} = 8080$ and $\gamma_{1,2} = 5 \times 10^{-4}$.

Nusselt number of fluid phase in the porous layer which is shown in Fig. 11 is less than the Nusselt number of the solid phase by 99.9 %. This notable difference is mainly due to the very high thermal conductivity ratio between the foam and the fluid saturated in it. The increase of Da increases the Nu for high values of Re. The increasing of Re provides the minimized viscous force and high penetration through the permeable foam.
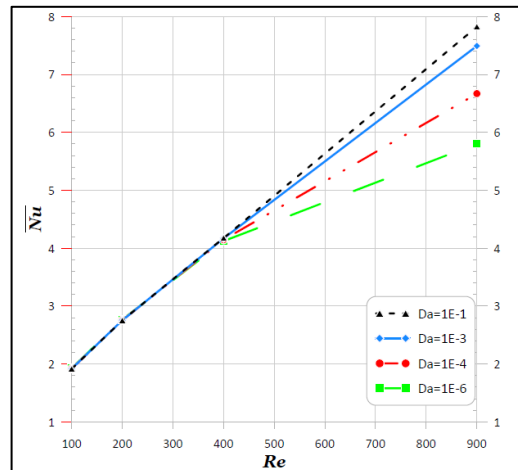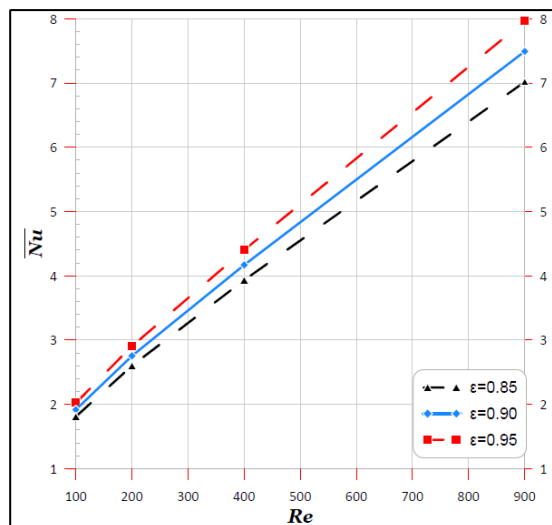

Fig. 11 Average Nu (fluid only) with Re for various Ri in porous media domain of $\varepsilon = 0.9$, $Da = 10^{-3}$, $Pr = 0.71$, $\sigma_{1,2} = 8080$ and $\gamma_{1,2} = 5 \times 10^{-4}$.

Fig. 12 shows the average Nusselt number (solid and fluid phases) with Reynolds numbers for various porosities of porous media domain. The decreasing in porosity enhances heat transfer, where the heat transfer rate improves by 100 % when the porosity is change from $\varepsilon = 0.95$ to 0.9 at $Re = 100$-900 and by 50 % when the porosity is change from $\varepsilon = 0.9$ to 0.85. The presence of high porosity metal foam porous media enhances the heat transfer area up to point making the better contact with cold and hot fluid particles. This continues increase of this percentage results reverse proportional with average Nusselt number. The increasing of velocity making additional mixing which in turn improves heat transfer characteristics. The jet inlet stream position in parallel to porous media domain develops the significant inertial forces for various Re and porosity.

Fig. 12 Average Nu (fluid and solid phase) with Re for various ε in porous matrix domain for $Ri = 0.1$, $Da = 10^{-3}$, $Pr = 0.71$, $\sigma_{1,2} = 8080$ and $\gamma_{1,2} = 5 \times 10^{-4}$.

Fig. 13 shows the variations of the average Nusselt number of the fluid phase with Reynolds for various ε in fluid domain. The porosity has, relatively, lower effect on heat transfer than the Reynolds number. The forced convection is the main controlled mechanism in free stream channel. The porosity of porous media does not manipulate the free stream because the resultant heat transfer in free stream is out of porous media domain.

Fig. 13 Average Nu (fluid only) with Re for various ε in porous media domain $Ri = 0.1$, $Da = 10^{-3}$, $Pr = 0.71$, $\sigma_{1,2} = 8080$ and $\gamma_{1,2} = 5 \times 10^{-4}$.

4. Conclusions

The numerical investigation of heat transfer characteristics of jet impinging flow inside a horizontal channel involving a heat sink covered by a metal foamed is successfully investigated in this paper. Within the foam layer, local thermal non-equilibrium is considered between the solid and fluid. The following concluding remarks are drawn from this study.

1. The warmer heat sink and porous media are shown lower Reynolds number while the cold ones are shown in $Re = 900$ due to the influence of jet impinging.
2. The decreasing in the porosity of the foam enhances heat transfer, where the heat transfer rate improves by 100 % and 50 % when the porosity is decreased from $\varepsilon = 0.95$ to 0.9 and from $\varepsilon = 0.9$ to 0.85, respectively.
3. The presence of high porosity metal foam porous media enhances the heat transfer area which making the better contact with cold and hot fluid particles. The thickness of the foam layer will be investigated in the next paper.

Nomenclature		
Symbol	**Description**	**Unit**
a_{sf}	Specific surface area.	$m^2.m^{-3}$
h_{sf}	Solid to fluid interstitial heat transfer coefficient.	$W.m^{-2}.°K^{-1}$
h_v	Modified volumetric solid to fluid heat transfer coefficient.	$W.m^{-3}.°K^{-1}$
H_v	Volumetric heat transfer coefficient. $H_v = h_v.w^2.k_f^{-1}$	-
K	Permeability.	m^2
Da	Darcy number, $Da = K/w_p^2$	-
Re	Reynolds number, $Re = v_{in}.w/v$	-
Pr	Prandtl number.	-
Pe	Peclet number, $Pe = v_{in}.w.\alpha^{-1}$	-
Gr^*	Modified Grashof number.	-
Ri	Richardson number, $Ri = Gr/Re^2$	-
$k_{f,s,hs}$	Fluid, solid matrix & heat sink thermal conductivity.	$W.m^{-1}.°K^{-1}$
w	Jet slot width.	m
W_p	Dimensionless porous layer width w_p/w	-
W_{ch}	Dimensionless channel width w_{ch}/w	-
H_p	dimensionless porous layer height h_p/w	-
H_{ch}	Dimensionless channel height h_{ch}/w	-
H_{hs}	Dimensionless heat sink height h/w	-
TB	Dimensionless substrate height tb/w	-
γ_1	Matrix to fluid thermal diffusivity ratio, $\gamma_1 = \alpha_s/\alpha_f$	-
Greek symbols		
Symbol	**Description**	**Unit**
ρ	Density.	$kg.m^{-3}$
μ	Dynamic viscosity.	$kg.m^{-1}.s^{-1}$
v	Kinematic viscosity, $v = \mu/\rho$	$m^2.s^{-1}$
θ	Non dimensional temperature	-
ε	Porosity, $\varepsilon = v_{voids}/v_p$	-
α	Thermal diffusivity.	$W.J^{-1}.m^{-1}$

$\alpha_{f,s,hs}$	Fluid, solid matrix & heat sink thermal diffusivity.	$W.J^{-1}.m^{-1}$
γ	Thermal diffusivity ratio.	-
σ	Thermal conductivity ratio.	-
β	Thermal expansion coefficient.	$°K^{-1}$
Subscripts		
Symbol	**Description**	**Unit**
f	Fluid.	-
s	Solid.	-
sf	Solid to fluid.	-
p	Porous.	-
hs	Heat sink.	-
ch	Channel.	-
1	Matrix to fluid.	-
2	Heat sink to fluid.	-
γ_2	Heat sink to fluid thermal diffusivity ratio, $\gamma_2 = \alpha_{hs}/\alpha_f$	-
σ_1	Matrix to fluid thermal conductivity ratio, $\sigma_1 = k_s/k_f$	-
σ_2	Heat sink to fluid thermal conductivity ratio $\sigma_2 = k_{hs}/k_f$	-
X, Y	Dimensionless horizontal and vertical coordinate, $X = x/w$, $Y = y/w$	-
u, v	Fluid velocity in horizontal and vertical direction.	$m.s^{-1}$
v_{in}	Inlet normal velocity	-
U, V	Dimensionless velocity in horizontal and vertical direction $U = u/v_{in}$, $V = v/v_{in}$	-
Acronyms		
FMF	Finned metal foam.	
$LTNE$	Local thermal non equilibrium.	

References

[1] D. A. Nield and A. Bejan, Convection in porous media, 3rd edition, New York, Springer, 2006.

[2] R. Viskanta, "Heat Transfer to Impinging Isothermal Gas and Flame Jets", Experimental Thermal and Fluid Science, Vol. 6, Issue 2, pp. 111-134, 1993. https://doi.org/10.1016/0894-1777(93)90022-B

[3] S. Polat, "Heat and Mass Transfer in Impingement Drying", Drying Technology, Vol. 11, Issue 6, pp. 1147-1176, 1993. https://doi.org/10.1080/07373939308916894

[4] S. Gururatana, "Heat Transfer Augmentation for Electronic Cooling", American Journal of Applied Sciences, Vol. 9, No. 3, pp. 436-439, 2012. https://doi.org/10.3844/ajassp.2012.436.439

[5] L. Andrei, C. Carcasci, R. Da Soghe, B. Facchini, F. Maiuolo, L. Tarchi, S. Zecchi, "Heat Transfer Measurements in a Leading Edge Geometry with Racetrack Holes and Film Cooling Extraction," ASME J. Turbomach, Vol. 135, Issue 3, pp. 1-11, 2013. https://doi.org/10.1115/1.4007527

[6] S. N. Kane, A. Mishra, and A. K. Dutta, "Preface: International Conference on Recent Trends in Physics (ICRTP 2016)", Journal of Physics: Conference Series, Vol. 755, No. 1, 2016. https://doi.org/10.1088/1742-6596/755/1/011001

[7] H. Iacovides, and B. E. Launder, "Computational fluid dynamics applied to internal gas-turbine blade cooling: a review", Vol. 16, Issue 6, pp. 454-470, 1995. https://doi.org/10.1016/0142-727X(95)00072-X

[8] B. Han and R. J. Goldstein, "Jet-Impingement Heat Transfer in Gas Turbine Systems," Annals of the New York Academy of Science, Vol. 934, Issue 1, pp. 147-161, 2001. https://doi.org/10.1111/j.1749-6632.2001.tb05849.x

[9] J. Ferraria, N. Lior, and J. Slycke, "An evaluation of gas quenching of steel rings by multiple-jet impingement", Journal of Materials Processing Technology, Vol. 136, Issue 1-3, pp. 190-201, 2003. https://doi.org/10.1016/S0924-0136(03)00158-4

[10] W. B. Wright, "An Evaluation of Jet Impingement Heat Transfer Correlations for Piccolo Tube Application", NASA Center for Aerospace Information, 42nd AIAA Aerospace Sciences Meeting and Exhibit, Reno, Nevada, 5-8 January 2004. https://doi.org/10.2514/6.2004-62

[11] D. Babic, D. B. Murray, and A. A. Torrance, "Mist jet cooling of grinding processes", International Journal of Machine Tools and Manufacture, Vol. 45, Issue 10, pp. 1171-1177, 2005. https://doi.org/10.1016/j.ijmachtools.2004.12.004

[12] C. Glynn, T. O'donovan, and D. B. Murray, "Jet Impingement Cooling", 2005.

[13] B. Agostini, M. Fabbri, J. E. Park, L. Wojtan, J. R. Thome, and B. Michel, "State of the Art of High Heat Flux Cooling Technologies", Heat Transfer Engineering, Vol. 28, Issue 4, pp. 258-281, 2007. https://doi.org/10.1080/01457630601117799

[14] M. A. Ebadian and C. X. Lin, "A Review of High-Heat-Flux Heat Removal Technologies", Journal of Heat Transfer, Vol. 133, Issue 11, pp. 1-11, 2011. https://doi.org/10.1115/1.4004340

[15] S. Hussain, M. A. Ismael, and A. J. Chamkha, "Impinging jet into an open trapezoidal cavity partially filled with a porous layer", International Communications in Heat and Mass Transfer, Vol. 118, 2020. https://doi.org/10.1016/j.icheatmasstransfer.2020.104870

[16] K. C. Wong and N. H. Saeid, "Numerical study of mixed convection on jet impingement cooling in an open cavity filled with porous medium", International Communications in Heat and Mass Transfer, Vol. 36, Issue 2, pp. 155-160, 2009. https://doi.org/10.1016/j.icheatmasstransfer.2008.10.008

[17] N. S. Gibanov, M. A. Sheremet, M. A. Ismael, and A. J. Chamkha, "Mixed Convection in a Ventilated Cavity Filled with a Triangular Porous Layer", Transport in Porous Media, Vol. 120, pp. 1-21, 2017. https://doi.org/10.1007/s11242-017-0888-y

[18] B. Buonomo, O. Manca, S. Nardini, and G. Lauriat, "Numerical investigation on thermal and fluid dynamic behavior of laminar slot-jet impinging on a surface at uniform heat flux in a confined porous medium in local thermal non-equilibrium conditions", ASME International Mechanical Engineering Congress and Exposition, Vol. 8A, pp. 1–11, 2014. https://doi.org/10.1115/IMECE2014-39783

[19] T. M. Jeng and S. C. Tzeng, "Numerical study of confined slot jet impinging on porous metallic foam heat sink", International Journal of Heat and Mass Transfer, Vol. 48, Issue 23-24, pp. 4685-4694, 2005. https://doi.org/10.1016/j.ijheatmasstransfer.2005.06.032

[20] A. Sivasamy, V. Selladurai, and P. Rajesh Kanna, "Mixed convection on jet impingement cooling of a constant heat flux horizontal porous layer", International Journal of Thermal Sciences, Vol. 49, Issue 7, pp. 1238-1246, 2010. https://doi.org/10.1016/j.ijthermalsci.2010.01.010

[21] P. A. K. Lam and K. A. Prakash, "A numerical investigation of heat transfer and entropy generation during jet impingement cooling of protruding heat sources without and with porous medium", Energy Conversion and Management, Vol. 89, pp. 626-643, 2015. https://doi.org/10.1016/j.enconman.2014.10.026

[22] N. H. Saeid, "Mixed convection jet impingement cooling of a rectangular solid heat source immersed in a porous layer", Journal of Porous Media, Vol. 18, Issue 4, pp. 401-413, 2015. https://doi.org/10.1615/JPorMedia.v18.i4.40

[23] I. W. Maid, K. H. Hilal, and N. S. Lafta, "Experimental study of heat transfer enhancement using porous media in double tube heat exchanger", AL-Taqani, Vol. 30, No. 1, pp. 44-59, 2017.

[24] J. Shi, G. Zheng, Z. Chen, and C. Dang, "Experimental study of flow condensation heat transfer in tubes partially filled with hydrophobic annular metal foam", International Journal of Heat and Mass Transfer, Vol. 136, pp. 1265-1272, 2019. https://doi.org/10.1016/j.ijheatmasstransfer.2019.03.039

[25] C. T. DeGroot, A. G. Straatman, and L. J. Betchen, "Modeling forced convection in finned metal foam heat sinks", ASME, Journal of Electronic Packaging, Vol. 131, Issue 2, pp. 1–10, 2009. https://doi.org/10.1115/1.3103934

[26] J. Wang, H. Kong, Y. Xu, and J. Wu, "Experimental investigation of heat transfer and flow characteristics in finned copper foam heat sinks subjected to jet impingement cooling", Applied Energy, Vol. 241, pp. 433-443, 2019. https://doi.org/10.1016/j.apenergy.2019.03.040

[27] H. F. Jasim, "Role of the Fluid-Structure Interaction for Mixed Convection in a Square Cavity", M.Sc. thesis, Mechanical Engineering Department, College of Engineering, University of Basrah, 2018.

[28] D. T. Yaseen and M. A. Ismael, "Effect of Deformable Baffle on the Mixed Convection of Non- Newtonian Fluids in a Channel-Cavity", Basrah Journal for Engineering Science, Vol. 20, No. 2, 2020. https://doi.org/10.33971/bjes.20.2.3

[29] A. Q. Abd Al-Hassan and M. A. Ismael, "Numerical study of double diffusive mixed convection in horizontal channel with composite open porous cavity", Special Topics & Reviews in Porous Media: An International Journal, Vol. 10, Issue 4, pp. 401-419, 2019. https://doi.org/10.1615/SpecialTopicsRevPorousMedia.2019029342

[30] F. T. Dórea and M. J. S. De Lemos, "Simulation of laminar impinging jet on a porous medium with a thermal non-equilibrium model", International Journal of Heat and Mass Transfer, Vol. 53, Issue 23-24, pp. 5089-5101, 2010. https://doi.org/10.1016/j.ijheatmasstransfer.2010.07.055

[31] H. J. Xu, L. Gong, C. Y. Zhao, Y. H. Yang, and Z. G. Xu, "Analytical considerations of local thermal non-equilibrium conditions for thermal transport in metal foams", International Journal of Thermal Sciences, Vol. 95, pp. 73-87, 2015. https://doi.org/10.1016/j.ijthermalsci.2015.04.007

[32] J. M. Smith, H. C Van Ness, and M. M. Abbott, Introduction to Chemical Engineering Thermodynamics, Sixth Edition, 2010. ISBN 10: 0000053759, ISBN 13: 9780000053756.

[33] J. P. Holman, Heat Transfer, 10th Edition, McGraw Hill, New York, 2010. ISBN 978-0-07-352936-3

[34] R. Kulkarni, "Natural convection in enclosures with localised heating and cooling," Ph.D. thesis, Department of Mechanical Engineering, University of Wollogong, 1998. https://ro.uow.edu.au/theses/1587